NRC Research Press

ARTICLE

Oxygen depletion in subarctic peatland thaw lakes[1]

Bethany N. Deshpande, Frédéric Maps, Alex Matveev, and Warwick F. Vincent

Abstract: Permafrost thawing and erosion results in the enrichment of northern lakes by soil organic matter. These allochthonous inputs favour bacterial decomposition and may cause the draw-down of dissolved oxygen to anoxic conditions that promote methanogenesis. Our objective in the present study was to determine the seasonal variations in dissolved oxygen in a set of permafrost peatland lakes in subarctic Quebec, Canada, and to relate these changes to metabolic rates, ice cover, and mixing. The lakes had high dissolved organic carbon concentrations, and their surface waters in summer had greenhouse gas concentrations that were up to one (CO_2) to three (CH_4) orders of magnitude above air-equilibrium values, indicating their strongly heterotrophic character. Consistent with these observations, the peatland lakes had elevated rates of bacterial production and oxygen consumption. Continuous measurements of oxygen by in situ sensors and of ice cover by automated field cameras showed that the lakes became fully anoxic shortly after freeze-up. The waters were partially re-oxygenated by mixing events in spring and fall, but in one lake, the bottom waters remained anoxic throughout the year. These observations provide a foundation for subsequent biogeochemical and modelling studies of peatland thaw lakes as an abundant class of Arctic freshwater ecosystems.

Key words: oxygen, permafrost, respiration, thaw lakes, thermokarst.

Résumé : Le dégel et l'érosion du pergélisol entraînent l'enrichissement des lacs du Nord en raison de l'apport de matière organique de sol. Ces apports allochtones favorisent la décomposition bactérienne et peuvent causer la diminution d'oxygène dissous jusqu'à des conditions anoxiques qui aident la méthanogénèse. Notre objectif en entreprenant cette étude était de déterminer les variations saisonnières d'oxygène dissous pour un ensemble de lacs de tourbière de pergélisol dans la région subarctique du Québec, Canada, et d'établir un rapport entre ces changements et les taux métaboliques, la couverture de glace et le mélange. Les lacs avaient des concentrations élevées en carbone organique dissous et en été leurs eaux de surface avaient des concentrations en gaz à effet de serre qui étaient jusqu'à un (CO_2) et à trois (CH_4) ordres de grandeur au-dessus des valeurs d'équilibre d'air, indiquant leur caractère fortement hétérotrophe. Conformément à ces observations, les lacs de tourbière avaient des taux élevés de production bactérienne et de consommation d'oxygène. Des mesures prises en continue d'oxygène au moyen de capteurs in situ et de couverture de glace au moyen de caméras automatisées de terrain ont indiqué que les lacs devenaient entièrement anoxiques peu de temps après le gel. Les eaux ont été partiellement ré-oxygénées au printemps et à l'automne en raison de phénomènes de mélange, mais dans un des lacs, les

Received 30 September 2016. Accepted 25 April 2017.

B.N. Deshpande, A. Matveev, and W.F. Vincent. Centre for Northern Studies (CEN), Takuvik Joint International Laboratory & Biology Department, Université Laval, Laval, QC G1V 0A6, Canada.
F. Maps. Québec-Océan, Takuvik Joint International Laboratory, Biology Department, Université Laval, QC G1V 0A6, Canada.
Corresponding author: Bethany N. Deshpande (email: bethanydeshpande@gmail.com).
[1]This article is part of a Special issue entitled "Arctic permafrost systems."
Warwick F. Vincent currently serves as an Associate Editor; peer review and editorial decisions regarding this manuscript were handled by Scott Lamoureux.

eaux de fond sont restées anoxiques tout au long de l'année. Ces observations constituent un fondement pour des études ultérieures de biogéochimie et de modélisation portant sur les lacs thermokarstiques de tourbière en tant que classe abondante d'écosystèmes arctiques d'eau douce.

Mots-clés : oxygène, pergélisol, respiration, lacs thermokarstiques, thermokarst.

Introduction

The dissolved oxygen pool in thermokarst lakes and ponds (hereafter referred to as thaw lakes) is primarily controlled by three simultaneous and interacting processes: (1) consumption of oxygen by respiration, (2) production of oxygen by photosynthesis, and (3) gas exchange with the atmosphere (del Giorgio and Williams 2005; Holtgrieve et al. 2010). Respiration and primary production are controlled by a combination of biological, chemical, and physical variables, while atmospheric gas exchange is a physically mediated process. Respiration in lakes is subject to biological controls such as the biomass of respiratory organisms and the production of organic substrates for decomposition, chemical controls via the availability of nutrients and electron acceptors such as oxygen, and physical controls such as temperature, mixing, and exchanges of organic substrates and electron acceptors with the surrounding catchment and atmosphere.

In thaw lakes, organic matter is known to be mainly of allochthonous origin, as a result of erosion of the surrounding permafrost soils (Olefeldt and Roulet 2012). This provides substrates for bacterial heterotrophic production and also includes high concentrations of coloured dissolved organic matter (CDOM) that strongly attenuate light throughout the water column (Watanabe et al. 2011), thereby reducing autotrophic phytoplankton production at depth (Shirokova et al. 2009; Forsström et al. 2013; Roiha et al. 2015). Subarctic permafrost peatland lakes are favorable to both particle-based and free-living aquatic bacterial communities due to their high carbon and nutrient availability (Deshpande et al. 2016).

Temperature plays a key role in affecting oxygen dynamics in lakes and is especially important in cold environments such as Arctic and subarctic permafrost waters (Vonk et al. 2015). On a seasonal timescale, temperature influences the duration and thickness of ice cover, which limits the flux of oxygen from the atmosphere to the surface waters of the lake. With warmer temperatures, shorter ice-cover durations will extend the period of oxygen transport across the atmosphere–water interface, as has been shown in north-temperate lake ecosystems (Fang and Stefan 2009). At the same time, increased temperature may increase the rate of permafrost thaw and erosion of permafrost soils into thaw lakes, thereby increasing the availability of organic matter for decomposition processes (Olefeldt and Roulet 2012) as well as directly stimulating bacterial respiration.

Climate warming is predicted to influence ice- and snow-cover conditions that would subsequently impact the energy balance and biogeochemical processes of aquatic ecosystems in cold regions. For example, ice and snow thickness control the availability of light to phytoplankton and thereby affect autotrophic biomass and oxygen production (Vincent et al. 2013). The melting of snow and ice represents a positive feedback loop for warming, with modelling predictions generally showing earlier ice break-up dates and later freeze-up dates for lakes in the North American Arctic (Graversen et al. 2008; Brown and Duguay 2011). Analysis of multiple data sets has revealed a continuous and substantial reduction in spring snow cover extent over a 30 year period throughout the Arctic (Brown et al. 2010), and the predicted shift towards a rainfall-dominated precipitation regime later this century will accelerate ice-melt and landscape erosion (Vincent et al. 2017).

Changes in ice and snow cover can result in pronounced ecological and biogeochemical changes within lakes (Prowse et al. 2011) and provide a valuable set of indicators for the use of lakes as sentinels of global change (Vincent et al. 1998; Williamson et al. 2009).

However, Arctic and subarctic systems are typically difficult to monitor because of their remote locations. As a result, several studies have explored the potential influences of climate change on aquatic ecosystems by employing a modelling approach. Modelling offers the ability to explore potential future changes in these complex ecosystems and to closely investigate present and future control variables. For example, Fang and Stefan (2009) modelled the effects of warming on temperature, ice cover, and oxygen dynamics in 27 small lakes in the United States and showed a warmer water column, a greater period of stratification in summer, and loss of ice thickness. Application of an ecological model to evaluate the controlling factors of hypoxia in the St. Lawrence Estuary revealed the importance of both pelagic and benthic respiration (Bourgault et al. 2012). Similarly, modelling of temperature, dissolved oxygen, and dissolved organic carbon (DOC) has been used an approach to evaluate the potential impacts of "browning" (increased DOC inputs) on boreal lake oxygen dynamics (Couture et al. 2015).

In addition to modelling, other approaches are now becoming increasingly possible for monitoring Arctic and subarctic lakes in the face of rapid climate change. The advent of high-resolution automated oxygen sensors has provided opportunities to measure key metabolic variables by way of continuous, high-frequency measurements (Staehr et al. 2010). Automated time-lapse photography has provided information about the timing and rates of permafrost change in Arctic ecosystems (van Everdingen and Banner 1979; Wobus et al. 2011), and the availability of such imagery is becoming more widespread.

The overall aim of the present study was to examine the effects of ice cover, stratification, and mixing on seasonal changes in underwater dissolved oxygen concentrations and specifically to extend our previous results (Deshpande et al. 2015) to focus on thaw lakes that occur in permafrost peatlands. This is a major class of thermokarst systems that has received relatively little attention to date, but the waterbodies of this type have been shown to have unusually high rates of methane emission to the atmosphere (Matveev et al. 2016). The study was undertaken in a peatland valley located near the village of Kuujjuarapik-Whapmagoostui (K-W) (55°17′N, 77°47′W) in subarctic Quebec. We profiled these remote lakes and measured their bacterial metabolic rates and the concentrations of greenhouse gases in summer. We used in situ sensors to measure temperature, oxygen, and conductivity throughout 1 year and used time-lapse photography for continuous observations of ice cover and snow depth. This produced a detailed, seasonal depiction of ice, thermal, and oxygen dynamics in peatland thaw lakes and provided a foundation for subsequent modelling studies of this biogeochemically active class of Arctic freshwater ecosystems.

Materials and methods

Study sites

We investigated five thaw lakes in a peatland valley to the north and south of the Sasapimakwananisikw River (hereafter referred to as SAS) (Fig. 1) near the village of K-W, which lies in northern Quebec. This region has experienced rapid climate change, including an increase in mean annual temperatures from –4.2 °C for 1932–1960 to –2.6 ± 1.2 °C for the period 2001–2010 (Bhiry et al. 2011). An additional 10 lakes in five other study sites were used for comparison purposes, including a rock-basin area unaffected by permafrost. The lakes lie along a gradient of continuous to sporadic permafrost spanning a total distance of more than 200 km (Fig. 1).

SAS is an area of sporadic permafrost with >50 organic-rich permafrost mounds (palsas) that are approximately 3–5 m in height and covered by a 60 cm soil active layer (Fig. 1) (Arlen-Pouliot and Bhiry 2005; Fillion et al. 2014). The vegetation is similar in the north (SAS2) and south (SAS1) areas and includes mixed shrubs and semi-aquatic plants, including

Fig. 1. Map of the six study regions including the SAS peatland valley (in bold).

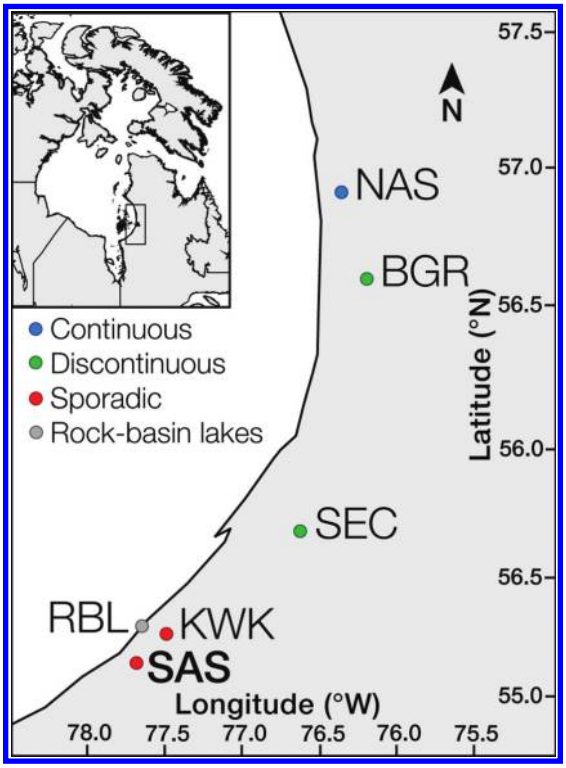

Carex aquatilis, *Carex rariflora*, *Eriophorum angustifolium*, and *Sphagnum* peat moss. The SAS valley contains many dark brown- and black-colored thaw lakes. Additional landscape details are shown in Fig. 7 of Vincent et al. (2017).

Of the additional study sites, two have lakes originating from lithalsa (inorganic permafrost mounds) degradation (KWK, NAS), while two other sites have thaw lakes originating from both palsa and lithalsa degradation (SEC, BGR). The KWK site is located within the valley of the Kwakwatanikapistikw River, located 8 km from SAS; it is an area of sporadic permafrost with numerous thaw lakes that vary in colour from blue-green to brown. The SEC and BGR1 study sites show similar colour variations to the KWK site and are in areas of discontinuous permafrost. SEC is located 86 km northeast of K-W and BGR is located in the Second River valley, near Hudson Bay and the village of Umijuaq. The Nastapoka River valley (NAS) is located to the north of BGR and contains clay-rich thaw lakes that were formed by thawing lithalsa mounds in this area of continuous permafrost. The thaw lakes studied are shallow (Z_{max} < 4.5 m) and have an average maximal diameter of ~30 m. The non-permafrost, rock-basin lakes included in the study were of similar area and depth (0.8–2.1 m) to the thermokarst systems but are underlain by rock rather than permafrost soils. Further information about the sites is given in Deshpande et al. (2016), with climate data for the SAS valley region in CEN (2017).

Lake sampling for limnological variables

Lakes were visited once each summer from 2012 to 2015; access to these remote sites was by helicopter based out of the CEN field station at K-W. At each visit, temperature, oxygen, pH, and conductivity were measured using a Hydrolab DS5X profiler (Loveland, Colorado).

Water samples were collected with a Van Dorn water bottle in the pelagic zone at the site of maximum depth and were analysed following Laurion et al. (2010) for total phosphorus (TP), total nitrogen (TN), DOC, chlorophyll *a* (Chl *a*), and total suspended solids (TSS). Bathymetric and morphometric data were provided from echo-sounding surveys by boat, and by aerial RGB photographs using an unmanned aerial vehicle, in a parallel study (G. Vieira and B. Deshpande, unpublished data).

Greenhouse gas measurements

Concentrations of CO_2 and CH_4 were measured in the surface waters of lakes in the SAS valley during summer 2013. Water was collected in 2 L LDPE bottles that were filled by submerging each bottle by hand beneath the surface, emptying and refilling twice, and ensuring no air bubbles were trapped in the bottle. The dissolved gases were extracted in situ as in Matveev et al. (2016): immediately after collection, 20 mL of water in the LDPE bottle was replaced by ambient air to create a headspace (100:1); the bottle was then vigorously shaken for 3 min to equilibrate the dissolved gases with the air, and then the headspace was subsampled. Ambient air samples were also taken directly in situ and stored overpressurized (10 mL of air in a 5.9 mL vial) in Labco Exetainer vials (Labco Limited, UK) sealed with butyl rubber stoppers. All samples were kept at cool temperature until laboratory analysis. Concentrations of CH_4 and CO_2 in the samples were determined in the laboratory by gas chromatography with flame ionization detection (Varian 3800, COMBI PAL head space injection system, CP-Poraplot Q 25 m) as in Bouchard et al. (2015).

Automated camera images of surface ice conditions

Photographs were captured from 4 September 2014 to 20 August 2015 for lakes SAS1A and SAS2A. Reconyx PC800 Professional cameras were installed at a distance of 5–10 m from the edge of each lake, taking six photographs every day at 1 h intervals between 10:00 a.m. and 15:00 p.m. Eastern Standard Time (EST). The cameras were protected in a metal housing at a height of 2–3 m above the ground. The full data set of these images is archived in Pienitz et al. (2017).

Automated in situ measurements

Mooring systems for lakes SAS1A, SAS1B, and SAS2A were constructed of chains and surface buoys. In SAS1A, two systems were installed from 25 August 2014 to 25 August 2015: one in the littoral zone and one in the pelagic zone. For the pelagic mooring, a subsurface float located 1.0 m below the air–water interface was used to keep the bottom set of sensors stable and reduce displacement ice during ice formation and break-up periods. Bottom weights resting on the lake sediments were attached to the pelagic subsurface float and to the littoral mooring system. In both SAS1B and SAS1A, a single mooring chain was installed in the deepest area of each lake. In lake SAS1B, the mooring went to a maximum depth of 1.0 m, with a surface float and bottom weights that rested on the sediments to keep the mooring in place. In SAS2A, the mooring was to a maximum depth of 2.5 m and included a subsurface float at a depth of 1.5 m and bottom weights as in the other systems. The following sensors were affixed to the rope by tie-wraps: dissolved oxygen and temperature loggers (DOT: MiniDO_2T optode systems, Precision Engineering, California; oxygen resolution 1.6 μg L^{-1}, temperature resolution 0.01 °C), conductivity and temperature loggers (CT: Hobo U24-001, Onset Computer Corporation, Massachusetts; conductivity resolution 1.0 μS cm^{-1}, temperature resolution 0.01 °C), and temperature loggers (T: Minilog-II-T; VEMCO/Amirix Systems, Nova Scotia; temperature resolution 0.01 °C). The logging frequency was set to 10 min for the oxygen optode (DOT) and temperature (T) sensors and 1.0 h for the conductivity (CT) sensors.

The configuration of the sensors was determined according to the summer water column profiles and to minimize freezing of the sensors. For the SAS1A deployment, DOT and CT loggers were installed at 0.7 and 1.2 m in the offshore pelagic zone and at a depth of 0.95 m in the inshore littoral zone. In SAS1B, T loggers were installed at depths of 0.25, 0.5, and 0.75 m, with DOT and CT loggers at the maximum depth of 1.0 m. In SAS2A, DOT and CT loggers were installed at 1.0 m and at 2.5 m depths.

Oxygen depletion rates

In situ oxygen depletion rates

In situ oxygen depletion rates were estimated based on changes in oxygen concentration during periods of darkness. These calculations are dependent on two major assumptions: first, that there is no photosynthesis during these overnight periods and, second, that nighttime respiration is equal to daytime rates (Staehr et al. 2010). Linear regression of oxygen concentrations during periods of temperature stability (i.e., when temperature SD < 0.1 °C) were used to determine oxygen consumption rates. In situ respiration rates were determined from the automated measurements of oxygen in SAS1A (littoral and pelagic) from midnight (0000) to 0500 each day (n = 30). Only rates with an R^2 value above 0.80 were used for further calculations.

In situ sediment oxygen consumption rates

Sediment chambers that measured 30.5 cm high with an 18 cm external diameter and a wall thickness of 0.2 cm (3/16 in.) were inserted into the sediments. They were sealed on top but open at the bottom and composed of a rigid, clear acrylic. One DOT logger (dissolved oxygen resolution 0.05 μmol L^{-1}, temperature resolution 0.01 °C) was installed inside each chamber and positioned ~5 cm over the lake sediments. Duplicate chambers were installed in the littoral zone of lake SAS1B and left for a total of 3 h, throughout which oxygen concentration and temperature were recorded every 10 min. SOC rates were determined via linear regression on the linear decreasing portion of the resulting curves, as in Utley et al. (2008).

Laboratory pelagic measurements

For measurements of pelagic oxygen concentrations overtime, triplicate samples were placed in glass vessels prefitted with an oxygen-sensitive optical sensor and sealed to inhibit gas transfer. A set of unsealed samples was also incubated and used to measure any potential temperature changes during measurement. For respiration rates, samples were incubated in the dark within a temperature-controlled circulating water bath at 15 °C. Oxygen concentration was measured using a fibre optic system (Fibox 3, PreSens Inc, Denmark). The Fibox probe was recalibrated every 24 h in one oxygen-free and one air-saturated environment. For each time point, the fluorescence-based probe was held to the sensor spot for approximately 1 min, measuring once every 4 s. The concentration of oxygen was measured every 6–8 h for 36–48 h. Oxygen consumption rates were determined via linear regression. Ten or more points were averaged for each of the time points. In the cases where an outlier skewed the regression, outlier points were removed until R^2 > 0.60.

Bacterial production

Bacterial production rates were measured via protein synthesis using radiolabelled [^{3}H]leucine incorporation (Kirchman 2001). Triplicate microfuge tubes plus a killed control were incubated, each containing 1.5 mL of sample and 40 nM of [4,5-^{3}H]leucine (60 Ci $mmol^{-1}$) (PerkinElmer Inc). Biomass production was terminated by the addition of 100 μL of trichloroacetic acid (100%) after 1 h and stored at 4 °C. Later, the samples were returned to the Takuvik Radio-isotope Laboratory at Université Laval where samples were processed using the centrifugation method of Smith and Azam (1992) and then radioassayed in a

scintillation counter to measure [^{3}H]leucine incorporation into protein. A conversion factor of 3.1 kg C mol leucine^{-1} was used to estimate net bacterial carbon production (Iriberri et al. 1990; Kirchman et al. 1993).

Statistical analysis

Limnological data were analysed via Pearson correlations using the R software package (R software v. 3.0.2, R Foundation for Statistical Computing, Austria). The relationships between bacterial respiration and production data with environmental variables were also examined by Pearson correlations. Bacterial production, respiration, and bacterial growth efficiency were analysed via one-way ANOVA to evaluate differences between the three lake groups: the SAS peatland lakes, thaw lakes from the other study sites, and the non-permafrost-affected rock-basin lakes (RBL) lakes. These analyses were performed using GraphPad Prism (v. 6.0f) (GraphPad Software Inc., California).

Results

Biogeochemical properties

The shallow (Z_{max} = 0.7–4.2 m) subarctic lakes studied were vertically stratified, with substantial differences in limnological properties between their surface and bottom waters (Table 1). DOC was on average twice as high in the SAS peatland lakes than in the other lakes studied, with an average (SD) of 15.8 (4.2) mg L^{-1} in SAS versus 8.3 (7.7) mg L^{-1} in the others. DOC was significantly negatively correlated with latitude ($r = -0.65$, $p < 0.05$) and positively correlated with longitude ($r = 0.68$, $p < 0.05$); southern lakes, such as the SAS peatland lakes and the KWK lithalsa lakes, tended to have more DOC than more northern lakes. Chl *a* values were lower in the SAS lakes, where the average (SD) was 4.1 (4.2) µg L^{-1}, than in the other thaw lakes that had an average (SD) of 10.0 (11.3) µg L^{-1}. TSS ranged from 1.8 to 810 mg L^{-1} in the full data set, with particularly high values in clay-rich NAS lakes (Table 1). The average (SD) TSS values in the SAS lakes were only 7.3 (5.6) mg L^{-1} and averaged 114 (229) (clearly not normally distributed) mg L^{-1} for all thaw lakes. TSS was correlated with SRP ($r = 0.78$, $p < 0.05$), particulate organic carbon (POC) ($r = 0.75$, $p < 0.05$), and TN ($r = 0.83$, $p < 0.05$) as well as with latitude ($r = 0.56$, $p < 0.05$) and longitude ($r = -0.44$, $p < 0.05$).

In the SAS valley peatland lakes, surface water concentrations in summer of CO_2 (SD) ranged from 127 (63) to 412 (123) µmol L^{-1}, equivalent to 7.3–23.8 times air-equilibrium concentrations (Table 2). Similarly, the surface concentrations of CH_4 (SD) ranged from 1.8 (1.0) to 11.3 (6.3) µmol L^{-1}, or 555–3410 times air-equilibrium values. These supersaturated concentrations indicated strong net fluxes of both gases, and especially CH_4, from the lakes to the overlying atmosphere.

Temperature, conductivity, and dissolved oxygen

Seasonal variations in SAS1A

In SAS1A, the offshore water column temperature was uniform from September to November 2014 (Fig. 2). It underwent cooling throughout this period, descending from a maximum of 14.9 °C on 31 August to 1.95 °C on 31 October. In early November, the water column then warmed from this minimum to the maximum winter temperature of 4.3 °C on 15 November. In winter, the surface layer at 0.7 m cooled more quickly than the bottom layer at 1.2 m and developed inverse temperature stratification that persisted throughout winter from mid-November 2014 until 24 April 2015. There was a maximum temperature difference between surface and bottom waters of 0.71 °C on 12 March. The thermal stratification was eliminated on 24 April 2015, when surface waters began to warm at the onset of spring. Throughout the spring and summer periods, from 24 April to the end of the record at 25 August 2015, several periods of thermal mixing were apparent, with water column temperatures increasing from a minimum of 0.5 °C to a maximum of 13.9 °C throughout this period.

Table 1. Limnological properties of the study sites.

Lake	Zm	Latitude (°N)	Longitude (°W)	Zs	TP	TN	DOC	SRP	Chl *a*	TSS	POC
SAS1A	1.6	55.218800	77.707950	S	17.8	0.59	13.1	< 3	2.97	4.65	2.73
SAS1B	1.2	55.219013	77.707801	S	17.8	0.82	18.8	< 3	1.99	5.75	3.08
SAS2A	2.7	55.225018	77.696580	S	13.4	0.66	13.7	3.0	3.58	2.17	1.34
				O	13.7	0.65	14.2	< 3	14.2	2.80	1.84
SAS2B*	1.5	55.225212	77.696017	S	15.1	0.61	12.8	1.12	4.21	6.00	3.00
				B	56.8	1.88	22.0	8.34	3.31	16.5	8.25
SAS2C*	2.1	55.225083	77.694933	S	17.2	0.59	11.0	1.03	1.58	4.62	2.31
				B	43.7	1.71	21.0	5.76	0.82	15.8	7.90
KWK1	2.7	55.330799	77.502767	S	467	1.08	16.9	5.0	8.71	13.8	2.64
				B	54.1	0.94	11.8	10.8	19.1	188	17.7
KWK11	1.6	55.330250	77.503367	S	118	1.01	26.5	< 3	23.9	8.32	4.09
				B	16.2	0.57	17.8	< 3	39.4	26.4	17.9
KWK12*	2.7	55.330072	77.503849	S	24.5	0.41	6.3	0.41	5.57	2.43	1.24
				B	71.1	0.63	7.6	1.78	4.99	6.11	5.04
SEC*	4.2	55.701033	76.643850	S	20.0	0.26	2.9	0.75	1.73	6.72	2.02
				B	82.5	0.35	3.9	1.56	12.5	61.6	18.5
BGR1*	4.1	56.610833	76.215000	S	11.6	0.24	2.4	0.42	0.98	1.97	0.58
				B	55.6	0.51	3.2	2.06	4.56	13.8	3.20
NAS1A	3.0	56.923779	76.378293	S	133	4.22	3	2.9	2.97	319	17.4
				B	175	4.14	2.1	19.2	1.99	810	26.0
NAS1H	3.6	56.924121	76.377038	S	30.5	0.602	4.1	6.2	3.58	18.20	9.10
RBL4K	0.7	55.331798	77.699393	S	12.1	0.63	5.9	5.9	14.2	1.79	0.91
				B	12.0	0.81	5.8	5.4	4.21	1.84	1.03
RBL 9K*	1.2	55.361083	77.650861	S	7.38	0.54	10.2	3.66	3.31	1.79	0.91
OLSHA	1.5	55.282452	77.739834	S	19.8	0.63	11.4	< 3	1.58	2.64	1.11

Note: Zm, maximum depth (m), location given by latitude and longitude, Zs, sample depth, total phosphorus (TP) (μg L^{-1}), total nitrogen (TN) (mg L^{-1}), dissolved organic carbon (DOC) (mg L^{-1}), soluble reactive phosphorus (SRP) (μg L^{-1}), chlorophyll *a* (Chl *a* (μg L^{-1}), total suspended solids (TSS) (mg L^{-1}), and particulate organic carbon (POC) (mg L^{-1}). The S samples correspond to surface at 0 m and the B samples correspond to the maximum depth of each lake. O corresponds to oxycline, at a depth of 0.5 m in SAS2A.
*Data are from Deshpande et al. (2016), with data collected during summer 2014. All other data are from summer 2015.

Table 2. Surface water concentrations of CO_2 and CH_4 in the SAS valley lakes.

Lake	Date	*n*	CO_2 (μmol L^{-1})	*R*	CH_4 (μmol L^{-1})	*R*
SAS1A	2 August 2013	4	127 (63)	7.3	2.2 (2.1)	658
SAS1B	30 July 2013	3	412 (123)	23.8	11.3 (6.3)	3410
SAS2A	3 August 2013	18	341 (85)	19.6	1.8 (1.0)	555
SAS2B	5 August 2013	14	277 (92)	16.0	3.5 (2.0)	1064
SAS2C	4 August 2013	14	250 (71)	14.0	2.1 (1.5)	624

Note: Values are the averages of *n* observations (SD in parentheses). *R* values are the ratios of measured mean concentration in the surface water to the calculated air-equilibrium concentration for the gas based on its measured concentration in the air over the lakes and its solubility at ambient temperatures.

The conductivity probes showed the presence of salinity differences throughout the surface and bottom waters of lake SAS1A throughout the full annual record, with the exception of spring mixing (Fig. 2). There was a difference of around 40 μS cm^{-1} at the end of August until 31 October. Conductivity increased throughout winter, extending from 40.8 to 202 μS cm^{-1} in the surface waters and from 1.2 to 172 μS cm^{-1} in the bottom waters. By the end of winter, the difference in conductivity between surface and bottom waters had decreased to around 30 μS cm^{-1}. In spring, there was a rapid and sudden drop in conductivity on 24 April that persisted until 2 May. In the surface layers,

Fig. 2. Seasonal variations in oxygen, conductivity, and temperature in the pelagic and littoral zones of SAS1A from summer 2014 to 2015.

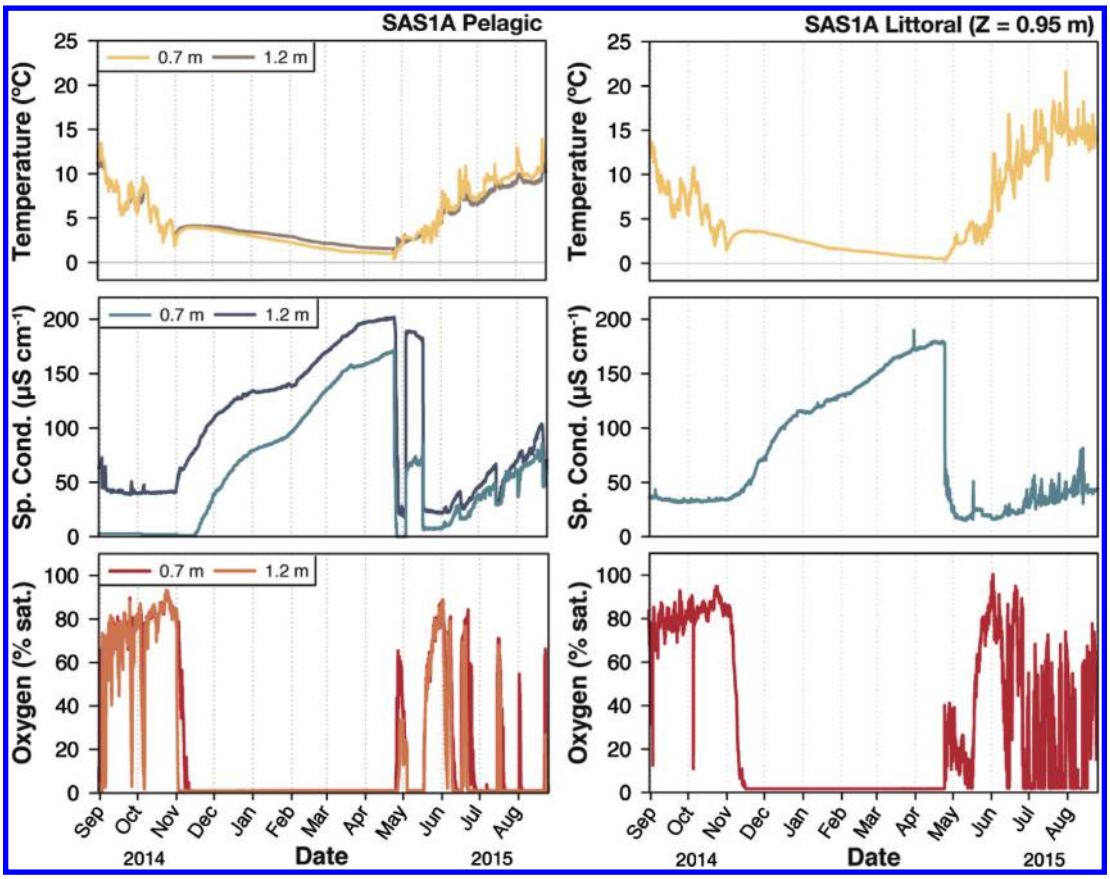

conductivity dropped from 171 to 0 (below detection) µS cm^{-1} and in the bottom waters, this drop was from 200 to 26.5 µS cm^{-1}. On 3 May, conductivity increased rapidly again, returning to similar levels of 188 µS cm^{-1} at 1.2 m, but only to 63.5 µS cm^{-1} at surface. These surface conductivity levels were approximately 100 µS cm^{-1} less than prior to the decrease. Later in spring, conductivity levels in the surface and bottom waters became more similar, suggesting intermittent mixing.

The oxygen data showed evidence of full water column mixing throughout fall, from the beginning of the record on 25 August to 31 October (Fig. 2). Beyond this period, bottom water oxygen levels dropped to 0% by 2 November and surface water oxygen dropped to 0% by 10 November 2014. This was equivalent to an oxygen depletion rate of 1.26 mg O_2 L^{-1} d^{-1} for the surface waters and 4.57 mg O_2 L^{-1} d^{-1} for the bottom waters. The pelagic water column remained anoxic throughout winter from 10 November 2014 to 24 April 2015. The onset of spring mixing was evident on 25 April 2015, when oxygen saturation levels rose to 65% at 0.7 m depth and 33% at the bottom 1.2 m depth. In spring, there was a total of six reoxygenation events, where oxygen saturation levels rose above 50% in the surface waters and above 25% in the bottom waters. A reoxygenation event was also observed in the surface waters on 1 August 2015, but no effect was observed at the lake bottom.

The automated camera imagery at each of the sites confirmed that the sensor system remained in a stable position in SAS1A (Fig. 3). Based on these images, the ice-on date

Fig. 3. Site photographs recorded in SAS1A from fall 2014 to summer 2015. The photographs span the full annual cycle and show the abundant *Carex* growth in the lake littoral zones. Ice cover began to form on 1 November 2014 (top right panel) and began to melt on 25 April 2015 (second right panel).

was 1 November 2014, when air temperatures first dropped below 0 °C. Ice thaw began on 25 April 2015 and continued until mid-May. The first date in 2015 when ice could no longer be seen on the surface of the lake was 18 May.

Temperature patterns in the littoral zone of SAS1A (at 0.95 m depth) followed closely those observed in the pelagic zone (Fig. 2). One difference was the intense mixing observed in spring for the littoral zone that appears to be more attenuated in the middle pelagic area. Conductivity also followed similar patterns but the sudden drop in conductivity from 179 to 24.7 μS cm^{-1} that was observed at the end of winter occurs 1 week earlier, on 18 April 2015, than what was observed in the pelagic zone. Conductivity fluctuated after the ice-off period in spring, but not as greatly as offshore.

The oxygen regime observed in the littoral zone followed closely that observed at the pelagic site. The water column remained well oxygenated from 25 August to 31 October 2014, when oxygen levels began to drop. In the littoral zone, the oxygen levels decreased from 83% saturation on 31 October to 0% by 14 November. The littoral water column remained anoxic from this date until 19 April 2015, when spring mixing and reoxygenation began. From 19 April onwards, there were approximately 12 mixing events when oxygen rose above 50% saturation and then returned rapidly to 0%.

Seasonal variations in SAS1B

In SAS1B, the water column temperature was uniform throughout much of fall from the end of August until 31 October 2014 (Fig. 4). Throughout this period, temperature decreased from a maximum of 25.9 °C to a minimum of 1.12 °C. From 31 October to 4 November, temperatures increased at each of the measured depths and winter thermal stratification was initiated. The 1 m deep water column remained thermally stratified throughout winter from 4 November 2014 to 26 April 2015. Temperatures decreased steadily throughout this period, with much of the water column at temperatures <1 °C by the end of winter. Ice formed to 0.25 m depth by 17 December 2014 and to 0.5 m depth as of 4 February 2015. Ice thickness never reached 0.75 m, as the water column remained above 0 °C at this depth throughout winter. On 27 April, temperatures began rising steadily. The beginning of spring had some periods of thermal mixing, although stratification was reestablished rapidly and could be observed as of 31 May.

Conductivity at a depth of 1.0 m remained around 50 μS cm^{-1} from the beginning of the record at 30 August 2014 to the end of the fall period at 4 November 2014 (Fig. 4). In winter, conductivity rose to a maximum of 184 μS cm^{-1} on 26 April 2015. At the onset of spring, conductivity decreased rapidly, reaching a minimum of 28.4 μS cm^{-1} on 4 May 2015. Throughout spring, conductivity increased intermittently, although consistently returned to a minimum of approximately 40 μS cm^{-1}.

Oxygen saturation levels fluctuated rapidly throughout the fall period, ranging from a maximum of 75% to a minimum of 4.4% (Fig. 4). Oxygen levels dropped rapidly to 0% saturation on 4 November 2014. The bottom waters of SAS1B remained anoxic from this date until 4 May 2015, when they increased slightly to 5.5% saturation and then returned to 0% saturation again until 13 May 2015. Throughout spring, several periods of reoxygenation were observed, sometimes reaching as high as 61% saturation, with rapid deoxygenation shortly after. There were nearly a dozen such periods from 13 May 2015 until the end of the record on 25 August 2015.

Seasonal variations in SAS2A

In SAS2A, the temperature record showed strong stratification throughout most of the year (Fig. 5). The surface water temperature at the beginning of the record, on 25 August 2014, was 11.1 °C, while the temperature in the bottom waters was 5.4 °C. Throughout the fall period, the surface water temperature fluctuated and decreased, reaching a minimum of 2.8 °C on 31 October 2014. The bottom water temperature, at a depth of 2.5 m, fluctuated less than the surface waters, reaching 4.4 °C on 31 October 2014. During this fall period, surface and bottom water temperatures coincided with each other at various dates, such as around 19 September, around 1 October, and from 11 October to 30 October 2014. At the beginning of winter, surface water temperatures warmed from 2.8 °C on 31 October to 4.2 °C on 17 November. Only slight warming was observed in bottom water temperatures, from 4.4 to 4.7 °C on 10 November. Throughout winter, water temperatures decreased steadily, with surface waters cooling more rapidly than bottom waters. Surface waters reached a winter minimum temperature of 0.72 °C on 29 April 2015. The winter minimum temperature of the bottom water was 2.5 °C on 14 May. During spring, surface water temperature

Fig. 4. Seasonal variations in oxygen, conductivity, and temperature in the pelagic zone of SAS1B from summer 2014 to 2015. The oxygen and conductivity measurements were at a depth of 1.0 m.

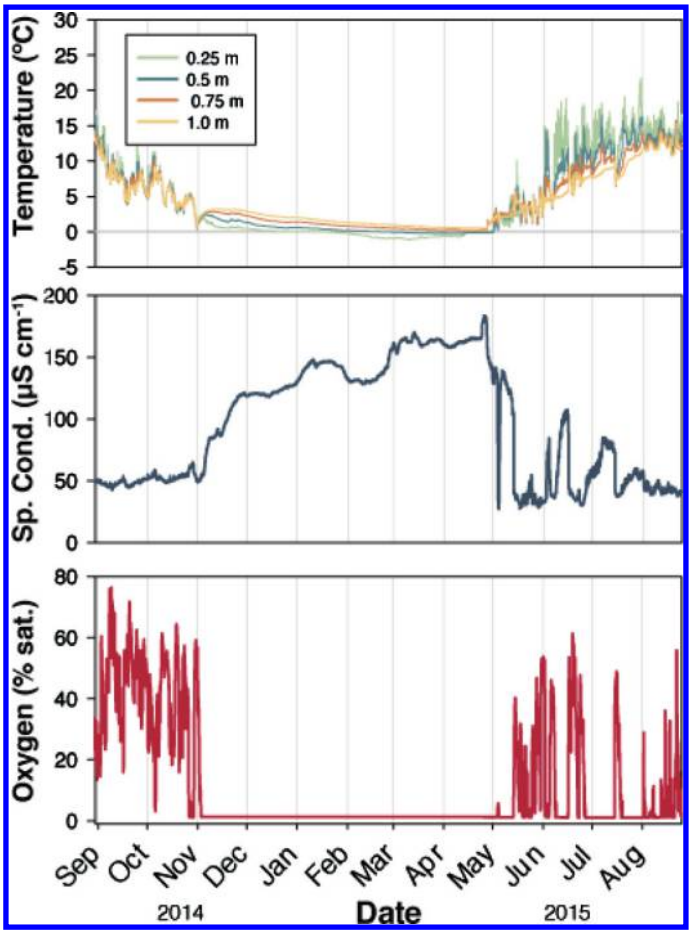

fluctuated and increased steadily, reaching 9.8 °C at the end of the record on 25 August. Bottom water temperatures increased as well, although at a much slower rate, reaching 5.1 °C on 25 August.

The surface and bottom water conductivities in SAS1A never coincided at any point throughout the full record, with an average difference of 180 µS cm^{-1}. Bottom water conductivities ranged from 172 to 278 µS cm^{-1}, while surface water conductivities ranged from 22 to 105 µS cm^{-1}. The minimum difference between the surface and bottom water records was 83 µS cm^{-1} on 5 March 2015.

As was observed in the annual conductivity record of this lake, oxygen also remained stratified throughout the full record (Fig. 5). In fall, oxygen saturation in the surface water fluctuated from a maximum of 40% saturation to a minimum of 0%. On 11 November 2014, the oxygen saturation at 1.0 m descended to 0%, where it remained throughout winter until 2 May 2015, when oxygen saturation increased to a spring maximum of 23%. Later in spring, there were three other sharp peaks of increased oxygen, but saturation remained under 6%. From 24 June 2015 until the end of the record on 25 August 2015, oxygen saturation at the 1.0 m depth was 0%. At the bottom 2.5 m depth, anoxia persisted throughout the full record. There was no evidence of reoxygenation or mixing of these bottom waters in spring; however, when the oxygen probe was recovered in summer 2015 and returned to

Fig. 5. Seasonal variations in oxygen, conductivity, and temperature in the pelagic zone of SAS2A from summer 2014 to 2015.

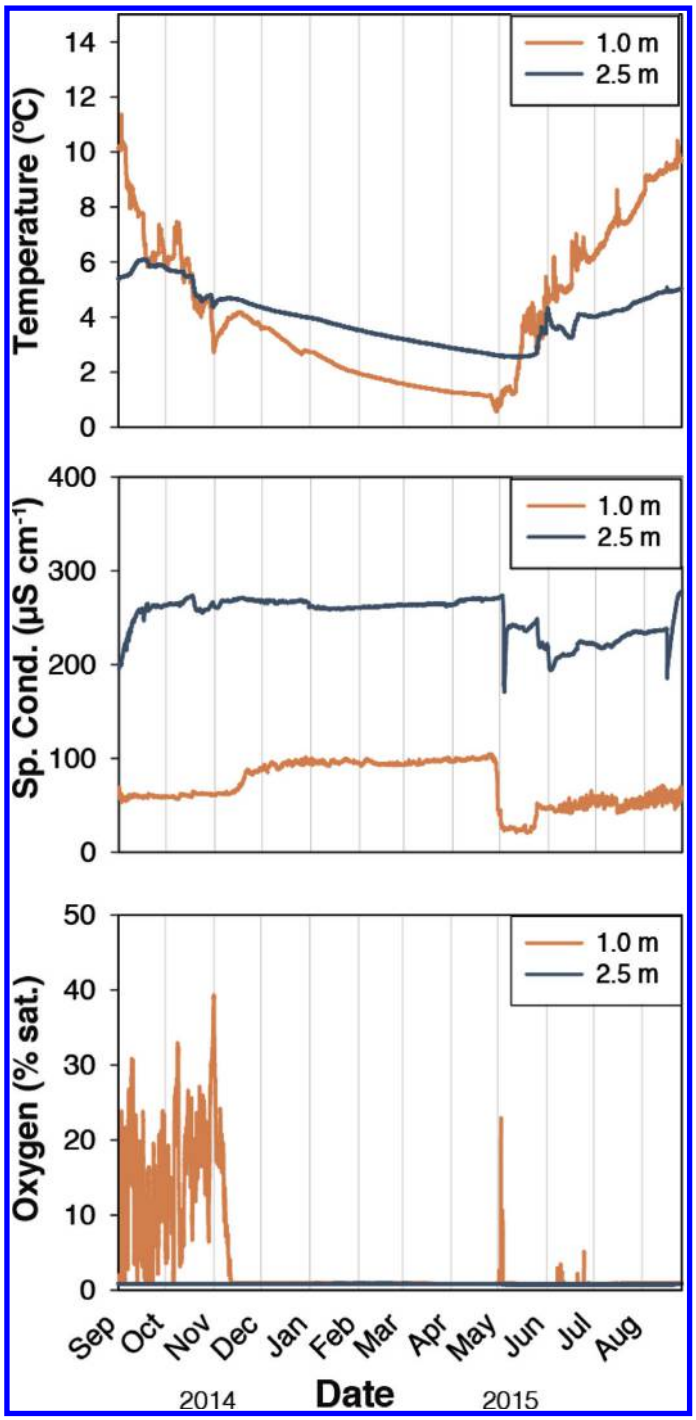

the surface, measured oxygen concentrations increased to 98.2% saturation, confirming that the sensor was still fully operational and had experienced minimal drift. The automated imagery at this site confirmed that the sensor system remained in a stable position in

SAS2A (Fig. 6). As in SAS1A, the ice-on date was 1 November 2014, while the ice-off date was slightly later, with full open water first observed on 22 May 2015.

Summer profiles

The SAS peatland thaw lakes were stratified in summer (Fig. 7). The dark colours of the lake surface warmed substantially, reaching more than 20 °C. All lakes were predominantly anoxic in summer, although anoxia was much more predominant in the SAS2 lakes than in SAS1. For example, in SAS2A, oxygen ranged from 106% at the surface and then decreased rapidly to 0% at 0.35 m, after which it was fully anoxic to the bottom depth of 2.7 m. SAS1A and SAS1B were both anoxic at bottom depths but remained oxygenated throughout a greater proportion of their water columns. For both SAS1 and SAS2 lakes, the surface waters were undersaturated in oxygen. In SAS2B, oxygen levels were only 45% of air equilibrium in surface waters. Conductivity increased substantially throughout the water columns of the SAS2 lakes; for example, in SAS2A, conductivity increased sixfold throughout the water column from 34.4 µS cm^{-1} in the surface to 209.5 µS cm^{-1} at depth. Conductivity of the SAS1 lakes was less variable throughout the water column; the total range of conductivity in SAS1A was from 42.9 to 45.6 µS cm^{-1}. Contrary to the permafrost peatland lakes, the non-thermokarst-affected lake RBL4K was well mixed and oxygenated throughout its entire water column.

In situ oxygen depletion rates

In situ oxygen depletion rates varied seasonally and also showed large differences between the upper and lower water columns in SAS1A (Fig. 8). Oxygen depletion rates were lowest in fall for the pelagic water column at 0.7 m and in the littoral zone at 0.95 m and increased in spring and summer. The opposite pattern was observed from the deeper 1.2 m sensor in the pelagic zone. At the 1.2 m depth, there was not the same magnitude of difference as observed from the other two sensors.

Bacterial metabolic activity

Respiration

Pelagic respiration rates ranged by an order of magnitude from a minimum of 0.079 to a maximum of 0.87 mg O_2 L^{-1} d^{-1} (Fig. 9). The average (SD) respiration rates in the SAS lakes were 0.46 (0.25) mg O_2 L^{-1} d^{-1}, while the averages (SD) in the other thaw lakes were 0.34 (0.28) mg O_2 L^{-1} d^{-1}. One-way ANOVA showed no statistically significant differences in respiration rates measured in the SAS lakes versus the other lake groups ($F(2,12) = 0.486$, $p = 0.63$). Bacterial respiration rates were correlated with Chl *a* values ($r = 0.455$, $p < 0.05$). The sediment oxygen uptake rates measured in SAS1B averaged (SD) 0.49 (0.17) g O_2 m^{-2} d^{-1}. This rate was adjusted for water column oxygen demand and resulted in an overall average (SD) of 0.26 (0.17) g O_2 m^{-2} d^{-1}.

Bacterial production

Bacterial production rates ranged from 0.236 to 1.83 µg C L^{-1} h^{-1} across the full data set (Fig. 9). The SAS lakes had an average (SD) rate of 0.72 (0.42) µg C L^{-1} h^{-1}, while the other thaw lakes had an average (SD) rate of 1.22 (0.31) µg C L^{-1} h^{-1}. One-way ANOVA showed statistically significant differences between bacterial production rates in the SAS lakes and other lake types studied ($F(2,12) = 4.195$, $p = 0.042$). Production rates were positively correlated with both DOC ($r = 0.63$, $p < 0.05$) and Chl *a* ($r = 0.41$, $p < 0.05$).

Discussion

Our in situ observations showed that the peatland thaw lakes were predominantly anaerobic systems, with anoxic conditions present throughout much of the year (Figs. 2, 4, and 5).

Fig. 6. Site photographs recorded in SAS2A from fall 2014 to summer 2015. The photographs span the full annual cycle and show the abundant *Carex* growth in the lake littoral zones. Ice cover began to form on 1 November 2014 (top right panel) and began to melt on 24 April 2015 (third left panel). By 22 May 2015, there is no more ice (third left panel).

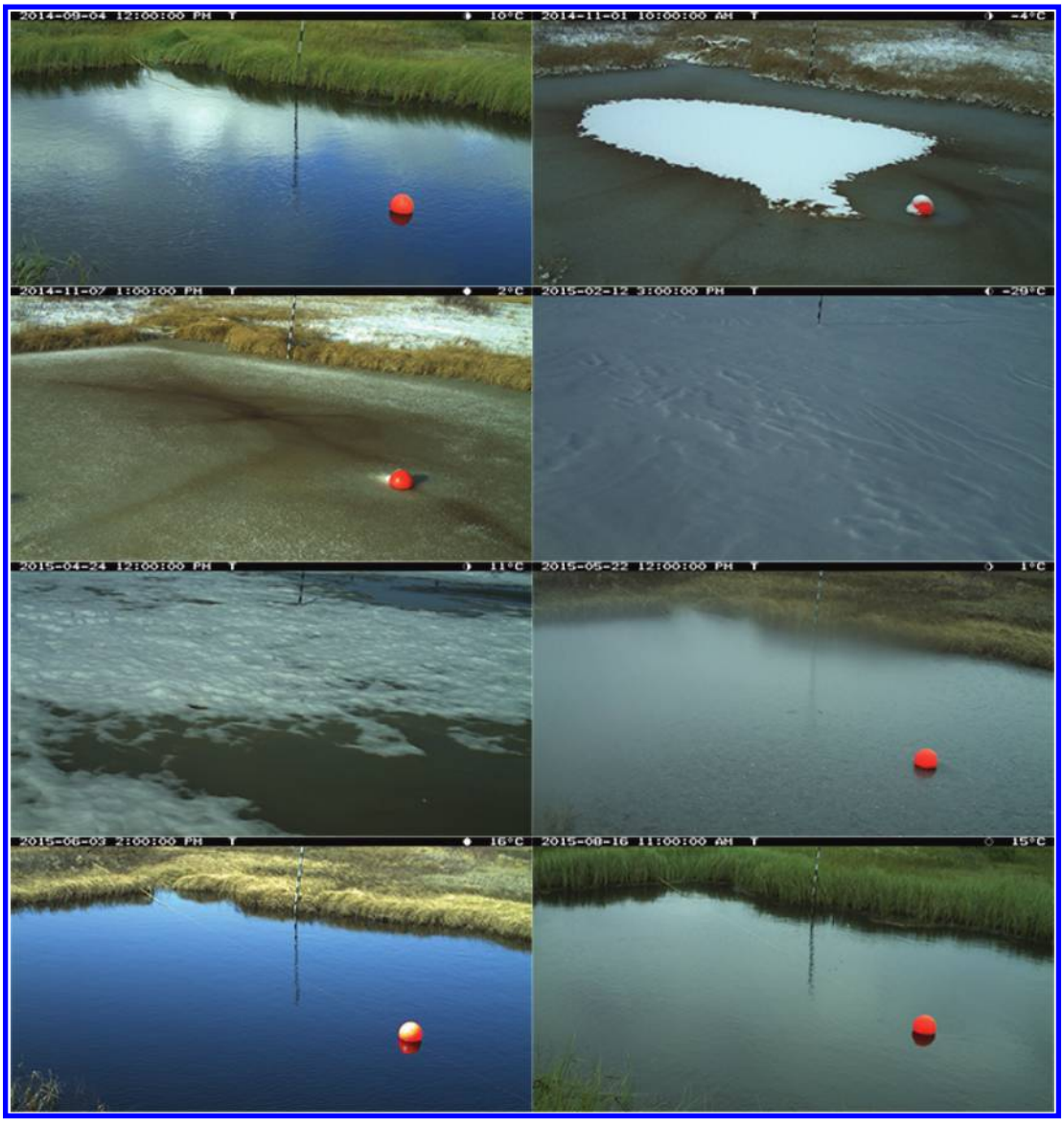

These observations are consistent with the highly supersaturated values of CO_2 and CH_4, which imply elevated rates of microbial decomposition, and redox conditions that are conducive to methanogenesis. These results build upon our observations from other sites in this region, and they reinforce earlier evidence of the tendency of these waters to be well stratified in summer despite their shallow depths (Laurion et al. 2010; Deshpande et al. 2015).

One of the most striking observations from the present data set is that lake SAS2A remained stratified throughout the year, with mixing never extending to the bottom of the lake in either spring or autumn (Fig. 5). Meromixis is typically thought of as a

Fig. 7. Water column profiles of temperature, specific conductivity, and oxygen saturation in five SAS lakes and one rock-basin lake. The dates of sampling were 26 June 2014 (SAS1A, SAS2A), 27 June 2014 (SAS1B), 29 June 2014 (SAS2B, SAS2C), and 7 July 2014 (RBL4K).

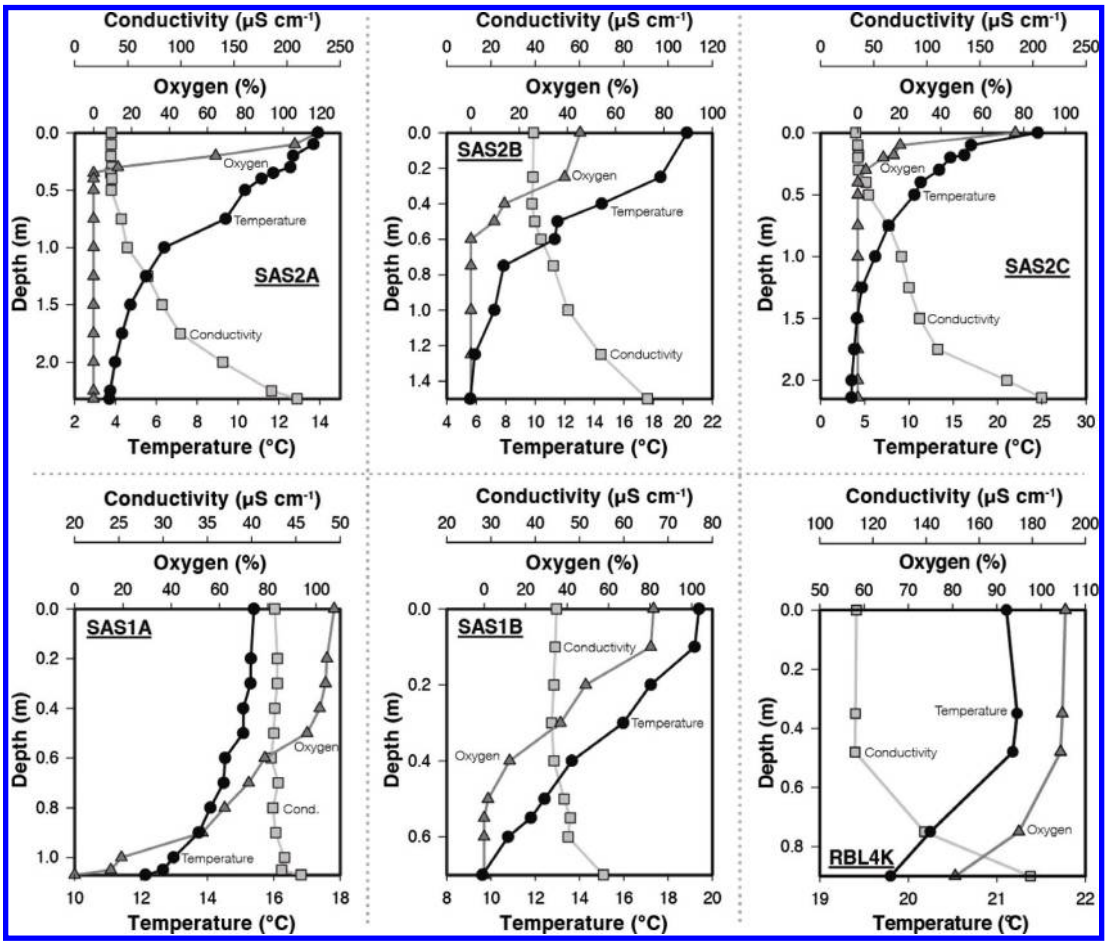

limnological feature of larger lakes that are permanently stratified as a result of highly saline bottom waters, for example, derived from ancient seawater (e.g., Van Hove et al. 2006). In peatland permafrost lakes, the observed meromixis is likely the result of the short fetch length, rapid warming of the strongly light-absorbing CDOM-rich surface waters, and the accumulation of stabilizing solutes in the bottom waters of the lake by freeze concentration and bacterial mineralization processes. This water column stability favours prolonged anoxia and net emission of CH_4 throughout the open water period.

The concentration of dissolved oxygen within each lake is likely controlled by a combination of physical, biological, and chemical factors that vary at daily, seasonal, and annual timescales. In these lakes, bacterial respiration associated with degradation of autochthonous and allochthonous (especially) organic matter exerts a major control on oxygen depletion rates. Physical aspects including advection, turbulent diffusion, and lake morphometric characteristics are also likely to act as control factors: the distinct seasonal oxygen variations observed in SAS1 lakes in contrast with those of SAS2A, despite similar biological characteristics, point to the role played by various physical factors such as lake basin shape.

Fig. 8. In situ oxygen depletion rates in SAS1A in the pelagic area of the lake at depths of 0.7 and 1.2 m and in the littoral zone at a depth of 0.95 m. Depletion rates are broken into seasons, where fall is from the beginning of the record on 25 August to 1 November 2014, spring is 1 May to 30 June 2015, and summer is July 1 to the end of the record on 25 August 2015.

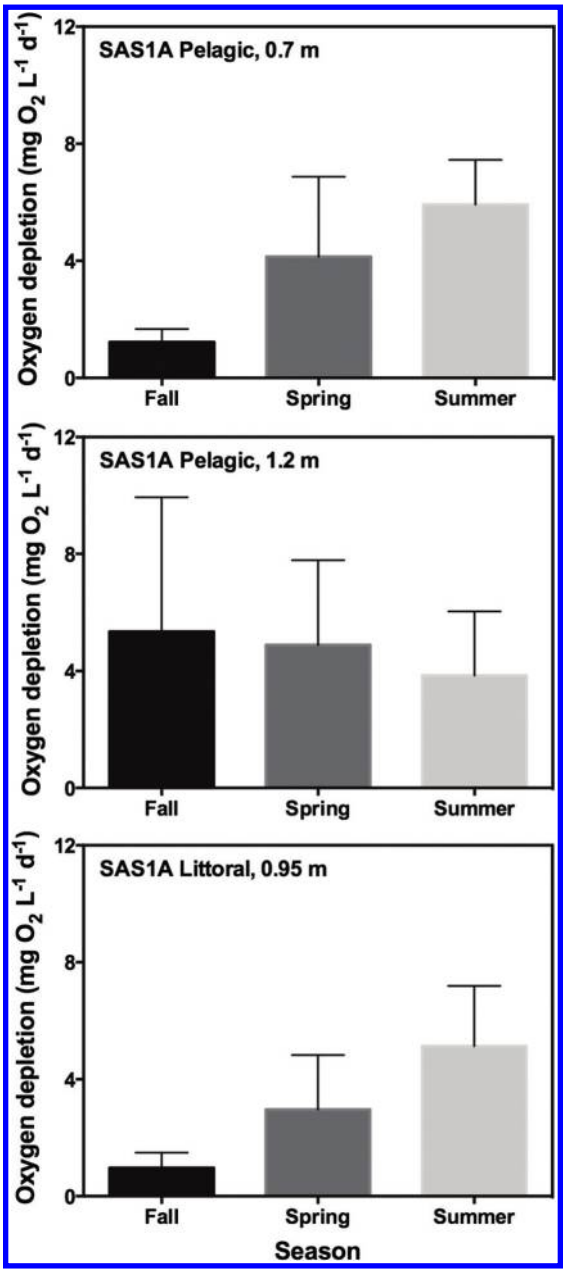

Oxygen depletion rates

For the wide range of sampled waterbodies, bottle measurements of bacterial respiration rates varied by an order of magnitude from 0.079 to 0.89 mg O_2 L^{-1} d^{-1}, with an average (SD) of 0.37 (0.24) mg O_2 L^{-1} d^{-1} (Fig. 9). These bacterial respiration rates are high in comparison with nonthermokarst Arctic or other subarctic lakes (Table 3). For example, respiration

Fig. 9. Bacterial respiration rates (BR) and bacterial production rates (BP) measured in bottle incubations of surface water samples from each of the study lakes.

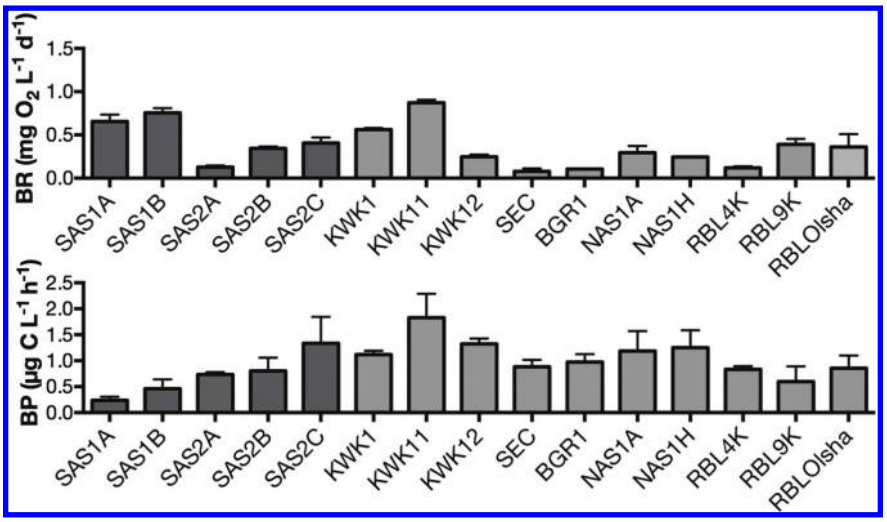

rates in these systems are two orders of magnitude greater than those recorded in ultraoligotrophic Toolik Lake (Lennon and Cottingham 2008) and more than 2.5 times greater than the maximum reported from a series of subarctic Swedish lakes (Jansson et al. 2008). These respiration rates are more within the range for mesotrophic lakes found in temperate regions (Biddanda et al. 2001; Hanson et al. 2003).

Oxygen depletion rates measured during periods of darkness from the in situ oxygen sensors showed higher rates than those measured during bottle experiments. This was as expected, since the in situ rates reflect the combined effect of physical, sediment, and planktonic processes operating in the lake, while the bottle experiments specifically target the plankton. The substantially higher rates in the lakes imply a much greater importance of sediment processes. There was also substantial seasonal variation: during fall, oxygen depletion rates in SAS1A were an average (SD) of 1.3 (0.4) mg O_2 L^{-1} d^{-1} at 0.7 m and 5.3 (4.6) mg O_2 L^{-1} d^{-1} at 1.2 m. The latter rate is comparable to in situ respiration rates measured in Crystal Bog, a shallow dystrophic lake in Wisconsin, where rates measured at the end of summer were approximately 4.6 mg O_2 L^{-1} d^{-1} (Hanson et al. 2008). In situ measures in a eutrophic lake and in an oligotrophic lake, both located in Wisconsin, showed rates of approximately 2 and 0.75 mg O_2 L^{-1} d^{-1}, respectively. While the in situ rates such as those determined from the mooring system in SAS1A are well above most bottle measurements, they are within the published range for north-temperate eutrophic lakes.

Bacterial respiration rates are controlled by the availability of organic substrates, the abundance of bacterial populations, and environmental factors such as temperature and availability of inorganic nutrients. In thermokarst thaw lakes, high concentrations of DOM, particularly of terrestrial origin, and substantial bacterial populations support high respiration rates (Rossi et al. 2013; Deshpande et al. 2016). Although DOC concentration has been identified as a main driver of interannual variations in oxygen content in other aquatic ecosystems, bacterial biomass and production in these peatland thaw lakes do not seem to be limited by organic carbon availability (Palmer et al. 2014; Deshpande et al. 2016). In humic lakes, it has been shown that high concentrations of DOC encourage a dominance towards chemoorganotrophic metabolic processes and away from autotrophic metabolic processes that would increase oxygen concentrations (Forsström et al. 2013). This phenomenon has been consistently observed in humic lakes of northern Sweden

Table 3. Comparison of oxygen consumption rates (mg O_2 L^{-1} d^{-1}) in thaw lakes versus other aquatic systems during summer.

Lake name	Location	Trophic status	Rate	Reference
Toolik Lake	Alaska	Oligotrophic	0.00123	Lennon and Cottingham 2008
Lake No. 16	Subarctic Sweden	High alpine	0.00219	Jansson et al. 2008
Jack Lake	Ontario	Mesotrophic	0.0270	Linsey and Lasenby 1985
Lake No. 10	Subarctic Sweden	Low alpine	0.0296	Jansson et al. 2008
BGR1	Northern Quebec	Thaw lake (oligotrophic)	0.106	This study
Chertsey	North of Montreal	Oligotrophic	0.115	Carignan et al. 2000
Violon Lake	North of Montreal	Oligotrophic	0.123	Carignan et al. 2000
SAS2A	Peatland lake, northern Quebec	Thaw lake (mesodystrophic)	0.128	This study
Lake No. 2	Subarctic Sweden	Coniferous forest	0.139	Jansson et al. 2008
Pin Rouge	North of Montreal	Oligotrophic	0.187	Carignan et al. 2000
KWK12	Northern Quebec	Thaw lake (mesotrophic)	0.247	This study
NAS1A	Northern Quebec	Thaw lake (mesotrophic)	0.296	This study
SAS2B	Peatland lake, northern Quebec	Thaw lake (mesodystrophic)	0.345	This study
SAS2C	Peatland lake, northern Quebec	Thaw lake (mesodystrophic)	0.406	This study
SAS1A	Peatland lake, northern Quebec	Thaw lake (mesodystrophic)	0.655	This study
SAS1B	Peatland lake, northern Quebec	Thaw lake (mesodystrophic)	0.755	This study
Round Lake	Minnesota	Mesotrophic	0.830	Biddanda et al. 2001
KWK11	Northern Quebec	Thaw lake (mesotrophic)	0.834	This study
SEC	Northern Quebec	Thaw lake (mesotrophic)	0.885	This study
Johanna Lake	Minnesota	Eutrophic	0.920	Biddanda et al. 2001
Cranberry Bog	Michigan	Mesotrophic	1.58	Hanson et al. 2003
Northgate bog	Michigan	Dystrophic	2.48	Hanson et al. 2003
Hummingbird Lake	Michigan	Eutrophic	4.67	Hanson et al. 2003

when DOC concentrations were equal to or greater than 10 mg L^{-1} (Jansson et al. 2000), as is the case for the peatland thaw lakes studied here (Table 1).

Sedimentary and hypolimnetic oxygen depletion is dependent upon temperature, hypolimnion thickness, and the supply of organic matter that is usually produced via photosynthesis within the surface water layers and transported to the hypolimnion via sinking and transport processes (Charlton 1980). Multiple studies have demonstrated the overall control of water column dissolved oxygen concentrations via bacterial consumption within sediments or at the water–sediment interface (Charlton 1980; del Giorgio and Williams 2005; Terzhevik et al. 2010). In permafrost peatland lakes, benthic biological processes may exert a control over CO_2 production in these lakes during oxic conditions (Laurion et al. 2010; Matveev et al. 2016). Sedimentary oxygen uptake in SAS1B was two times higher than pelagic bacterial community demand during oxygenated summer periods. In SAS1A, during the oxygenated fall period, in situ oxygen depletion rates were more than four times higher at a depth of 1.2 m than at the depth of 0.7 m (i.e., 5.3 mg O_2 L^{-1} d^{-1} at 1.2 m but only 1.2 mg O_2 L^{-1} d^{-1} at 0.7 m depth). However, these oxygen depletion rates do not act as a controlling factor throughout the full annual cycle. Peatland thaw lakes have hypoxic and anoxic bottom water conditions throughout most or even all (SAS2A) of the year. The sediment area to water volume ratios are higher than the range for other types of lakes reported in the literature (Mathias and Barica 1980; del Giorgio and Williams 2005). For example, the ratio of sediment area to water volume in is 0.9 m^{-1} in SAS1A, 2.7 m^{-1} for SAS1B, and 1.2 m^{-1} in deeper SAS2A (B. Deshpande and G. Vieira, unpublished data) versus maximum values of 0.42 m^{-1} in Lac Fraser,

Quebec (del Giorgio and Williams 2005), and up to a maximum of 0.64 m^{-1} for the north-temperate and Arctic lakes studied by Mathias and Barica (1980). Under winter conditions of ice and snow cover, dissolved oxygen concentrations are potentially controlled by either dissolved oxygen diffusion from the water column into bottom sediments or the rate of consumption by bacterioplankton in the process of organic matter mineralization or a combination of both processes (Terzhevik et al. 2010). The low water volume to high sediment area observed in thaw lakes, coupled with high rates of oxygen depletion within the hypolimnion, resulted in rapid deoxygenation of benthic waters within less than a week following the onset of ice cover (Figs. 2, 4 and 5). The bacterial populations remained at above-zero temperatures and do not seem to be strongly affected by the low water temperatures (~4 °C) at this time. Assuming that bacterial respiration processes would continue throughout the full range of winter temperatures, the anoxic conditions in these lakes are likely to be predominantly controlled by transport processes. As is most pronounced in deeper SAS2A, the lack of mixing and transport of oxygen throughout the water column results in persistent anoxic bottom water conditions throughout the annual cycle.

The littoral zones of these peatland permafrost lakes contain abundant plant life, with a strong seasonality of production and loss, as seen in the automated camera images (Figs. 3 and 6). *Carex* has colonized the shallow areas of SAS1A, representing an estimated 35% of the total lake area (Figs. 3 and 6; B. Deshpande and G. Vieira, unpublished data). Previous studies have observed higher concentrations of dissolved oxygen in littoral regions than pelagic, attributed to under-ice photosynthetic activity (Stefanovic and Stefan 2002). In other high-latitude lakes, solar radiation warms the water column through the ice, sometimes resulting in warming of the littoral zone in spring, even before air temperatures have increased above 0 °C (Terzhevik et al. 2010; Boike et al. 2015). In the permafrost peatland lakes studied here, it is likely that *Carex* respiration and decomposition contribute substantially to oxygen depletion at the onset of winter. *Carex* communities have been shown to have the highest respiration rates during initial decay when the most bioavailable compounds are rapidly decomposed (Aerts and de Caluwe 1997). This same study showed that *Carex* lost 50% of its dry mass via decomposition within the first 12 months after the onset of decay (Aerts and de Caluwe 1997). Site photographs of SAS1A show stark contrasts between decaying *Carex* during much of the year and green, photosynthetically active *Carex* during a short period of growth. From the set of in situ images, *Carex* grew from early June to early October each year but was richly green for less than 3 months of this period (Fig. 3). In spring, photosynthetic activity by *Carex* may partially explain the higher and more stable concentrations of dissolved oxygen observed in the littoral zone (Fig. 2). *Carex* has a low temperature optimum in cold environments, with ongoing photosynthesis by the leaves and oxygen consumption by the root systems even at near-frozen temperatures (Chapin and Oechel 1983). While photosynthetic activity by these aquatic plants may contribute to oxic conditions during certain parts of the year, the large quantity of degrading material may contribute to oxygen depletion processes throughout a more extended period of the year, which would also affect methane and CO_2 production within these lakes (Table 2).

Conclusions

Peatland thaw lakes are hotspots for microbial activity in subarctic tundra environments, with biogeochemical tendencies towards rapid oxygen depletion, anoxia, and greenhouse gas production. We observed large variations in oxygen depletion rates vertically with depth, horizontally between littoral and pelagic zones, and throughout the seasons on an annual cycle. The high oxygen demand of peatland thaw lakes is determined by

biological factors, notably by their elevated microbial production rates due to the influx of allochthonous organic matter from the eroding permafrost landscape (as indicated by their colour and high DOC concentrations) in combination with autochthonous carbon supplies, especially from the macrophyte communities that thrive in the littoral and supralittoral zones of the lakes. Oxygen consumption rates are likely to be limited by physical factors related to the transport of oxygen throughout the water column, notably the barrier to exchange with the atmosphere imposed by prolonged ice cover in the cold subarctic climate and the strong water column stability that resists mixing and reoxygenation during summer ice-free conditions. These highly stratified, oxygen-deficient waters are a distinctive class of northern freshwater ecosystems, and modelling efforts in the future should be directed towards understanding how their biogeochemical properties will respond to ongoing climate change.

Acknowledgements

This study was made possible with financial support from the Natural Sciences and Engineering Research Council of Canada (NSERC), the Canada Research Chair program, and the Quebec Nature and Technology Research funds (FRQNT). Financial and logistical support is further provided by the Centre for Northern Studies (Université Laval), the NSERC Discovery Frontiers grant ADAPT (Arctic Development and Adaptation to Permafrost in Transition), and the Northern Science Training Program. We thank P. Bégin, J. Comte, A. Matveev, A. Przytulska-Bartosiewicz, V. Mohit, D. Sarrazin, and C. Tremblay for their help in the field, J. Comte, F. Bruyant, and M.-J. Martineau for laboratory support and advice, and I. Laurion and J. Boike for their insightful feedback on this study. We thank S. Prémont at the INRS-ETE laboratory for support and guidance with sample analysis. We thank the Centre for Northern Studies field team for providing access to time-lapse imagery and meteorological data via the Nordicana D database. We thank G. Vieira and J. Canário for their comments on the manuscript and support in the field and for the use of unpublished UAV data. We thank the two anonymous reviewers for their insightful comments and suggestions.

References

Aerts, R., and de Caluwe, H. 1997. Initial litter respiration as indicator for long-term leaf litter decomposition of *Carex* species. Oikos. **80**: 353–361. doi: 10.2307/3546603.

Arlen-Pouliot, Y., and Bhiry, N. 2005. Palaeoecology of a palsa and a filled thermokarst pond in a permafrost peatland, subarctic Québec, Canada. Holocene. **15**: 408–419. doi: 10.1191/0959683605hl818rp.

Bhiry, N., Delwaide, A., Allard, M., Bégin, Y., Filion, L., Lavoie, M., Nozais, C., Payette, S., Pienitz, R., et al. 2011. Environmental change in the Great Whale River region, Hudson Bay: five decades of multidisciplinary research by Centre d'études nordiques (CEN). Ecoscience. **18**: 182–203. doi: 10.2980/18-3-3469.

Biddanda, B., Ogdahl, M., and Cotner, J. 2001. Dominance of bacterial metabolism in oligotrophic relative to eutrophic waters. Limnol. Oceanogr. **46**: 730–739. doi: 10.4319/lo.2001.46.3.0730.

Boike, J., Georgi, C., Kirilin, G., Muster, S., Abramova, K., Fedorova, I., Chetverova, A., Grigoriev, M., Bornemann, N., and Langer, M. 2015. Thermal processes of thermokarst lakes in the continuous permafrost zone of northern Siberia — observations and modeling (Lena River Delta, Siberia). Biogeosciences. **12**: 5941–5965. doi: 10.5194/bg-12-5941-2015.

Bouchard, F., Laurion, I., Prieskienis, V., Fortier, D., Xu, X., and Whiticar, M.J. 2015. Modern to millennium-old greenhouse gases emitted from ponds and lakes of the Eastern Canadian Arctic (Bylot Island, Nunavut). Biogeosciences. **12**: 7279–7298. doi: 10.5194/bg-12-7279-2015.

Bourgault, D., Cyr, F., Galbraith, P.S., and Pelletier, E. 2012. Relative importance of pelagic and sediment respiration in causing hypoxia in a deep estuary. J. Geophys. Res. **117**: C08033. doi: 10.1029/2012JC007902.

Brown, L.C., and Duguay, C.R. 2011. The fate of lake ice in the North American Arctic. Cryosphere. **5**: 869–892. doi: 10.5194/tc-5-869-2011.

Brown, R., Derksen, C., and Wang, L. 2010. A multi-data set analysis of variability and change in Arctic spring snow cover extent, 1967–2008. J. Geophys. Res. **115**: D16111. doi: 10.1029/2010JD013975.

Carignan, R., Planas, D., and Vis, C. 2000. Planktonic production and respiration in oligotrophic Shield lakes. Limnol. Oceanogr. **45**: 189–199. doi: 10.4319/lo.2000.45.1.0189.

CEN. 2017. Environmental data from Whapmagoostui-Kuujjuarapik Region in Nunavik, Quebec, Canada, v. 1.4 (1987–2016). Nordicana. **D4**: doi: 10.5885/45057SL-EADE4434146946A7.

Chapin, F.S., III, and Oechel, W.C. 1983. Photosynthesis, respiration, and phosphate absorption by *Carex aquatilis* ecotypes along latitudinal and local environmental gradients. Ecology. **64**: 743–751. doi: 10.2307/1937197.

Charlton, M.N. 1980. Hypolimnion oxygen consumption in lakes: discussion of productivity and morphology effects. Can. J. Fish. Aquat. Sci. **37**: 1531–1539. doi: 10.1139/f80-198.

Couture, R.-M., de Wit, H.A., Tominaga, K., Kiuru, P., and Markelov, I. 2015. Oxygen dynamics in a boreal lake responds to long-term changes in climate, ice phenology, and DOC inputs. J. Geophys. Res. Biogeosci. **120**: 2441–2456. doi: 10.1002/2015JG003065.

del Giorgio, P.A., and Williams, P.J.L.B. 2005. Respiration in aquatic ecosystems. Oxford University Press, New York.

Deshpande, B.N., MacIntyre, S., Matveev, A., and Vincent, W.F. 2015. Oxygen dynamics in permafrost thaw lakes: anaerobic bioreactors in the Canadian subarctic. Limnol. Oceanogr. **60**: 1656–1670. doi: 10.1002/lno.10126.

Deshpande, B.N., Crevecoeur, S., Matveev, A., and Vincent, W.F. 2016. Bacterial production in subarctic peatland lakes enriched by thawing permafrost. Biogeosciences. **13**: 4411–4427. doi: 10.5194/bg-13-4411-2016.

Fang, X., and Stefan, H.G. 2009. Simulations of climate effects on water temperature, dissolved oxygen, and ice and snow covers in lakes of the contiguous United States under past and future climate scenarios. Limnol. Oceanogr. **54**: 2359–2370. doi: 10.4319/lo.2009.54.6_part_2.2359.

Fillion, M.-E., Bhiry, N., and Touazi, M. 2014. Differential development of two palsa fields in a peatland located near Whapmagoostui-Kuujjuarapik, Northern Quebec, Canada. Arct. Antarct. Alp. Res. **46**: 40–54. doi: 10.1657/1938-4246-46.1.40.

Forsström, L., Roiha, T., and Rautio, M. 2013. Responses of microbial food web to increased allochthonous DOM in an oligotrophic subarctic lake. Aquat. Microb. Ecol. **68**: 171–184. doi: 10.3354/ame01614.

Graversen, R.G., Mauritsen, T., Tjernström, M., Källén, E., and Svensson, G. 2008. Vertical structure of recent Arctic warming. Nature. **451**: 53–56. doi: 10.1038/nature06502.

Hanson, P.C., Bade, D.L., Carpenter, S.R., and Kratz, T.K. 2003. Lake metabolism: relationships with dissolved organic carbon and phosphorus. Limnol. Oceanogr. **48**: 1112–1119.

Hanson, P.C., Carpenter, S.R., Kimura, N., Wu, C., Cornelius, S.P., and Kratz, T.K. 2008. Evaluation of metabolism models for free-water dissolved oxygen methods in lakes. Limnol. Oceanogr. Methods. **6**: 454–465. doi: 10.4319/lom.2008.6.454.

Holtgrieve, G.W., Schlinder, D.E., Branch, T.A., and A'mar, Z.T. 2010. Simultaneous quantification of aquatic ecosystem metabolism and reaeration using a Bayesian statistical model of oxygen dynamics. Limnol. Oceanogr. **55**: 1047–1063. doi: 10.4319/lo.2010.55.3.1047.

Iriberri, J., Unanue, M., Ayo, B., Barcina, I., and Egea, L. 1990. Bacterial production and growth rate estimation from [^{3}H]thymidine incorporation for attached and free-living bacteria in aquatic systems. Appl. Environ. Microbiol. **56**: 483–487.

Jansson, M., Bergström, A.-K., Blomqvist, P., and Drakare, S. 2000. Allochthonous organic carbon and phytoplankton/bacterioplankton production relationships in lakes. Ecology. **81**: 3250–3255. doi: 10.1890/0012-9658.

Jansson, M., Hickler, T., Jonsson, A., and Karlsson, J. 2008. Links between terrestrial primary production and bacterial production and respiration in lakes in a climate gradient in subarctic Sweden. Ecosystems. **11**: 367–376. doi: 10.1007/s10021-008-9127-2.

Kirchman, D.L. 2001. Measuring bacterial biomass production and growth rates from leucine incorporation in natural aquatic environments. Methods Microbiol. **30**: 227–237. doi: 10.1016/S0580-9517.

Kirchman, D.L., Keel, R.G., and Welschmeyer, N.A. 1993. Biomass and production of heterotrophic bacterioplankton in the oceanic subarctic Pacific. Deep Sea Res. Part 1. **40**: 967–988. doi: 10.1016/0967-0637(93)90084-G.

Laurion, I., Vincent, W.F., MacIntyre, S., Retamal, L., Dupont, C., Francus, P., and Pienitz, R. 2010. Variability in greenhouse gas emissions from permafrost thaw ponds. Limnol. Oceanogr. **55**: 115–133. doi: 10.4319/lo.2010.55.1.0115.

Lennon, J.T., and Cottingham, K.L. 2008. Microbial productivity in variable resource environments. Ecology. **4**: 1001–1014. doi: 10.1890/07-1380.1.

Linsey, G.A., and Lasenby, D.C. 1985. Comparison of summer and winter oxygen consumption rates in a temperate dimictic lake. Can. J. Fish. Aquat. Sci. **42**: 1634–1639. doi: 10.1139/f85-204.

Mathias, J.A., and Barica, J. 1980. Factors controlling oxygen depletion in ice-covered lakes. Can. J. Fish. Aquat. Sci. **37**: 185–194. doi: 10.1139/f80-024.

Matveev, A., Laurion, I., Deshpande, B.N., Bhiry, N., and Vincent, W.F. 2016. High methane emissions from thermokarst lakes in subarctic peatlands. Limnol. Oceanogr. **61**: S150–S164. doi: 10.1002/lno.10311.

Olefeldt, D., and Roulet, N.T. 2012. Effects of permafrost and hydrology on the composition and transport of dissolved organic carbon in a subarctic peatland complex. J. Geophys. Res. **117**: G01005. doi: 10.1029/2011JG001819.

Palmer, M.E., Yan, N.D., and Somers, K.M. 2014. Climate change drives coherent trends in physics and oxygen content in North American lakes. Clim. Change. **124**: 285–299. doi: 10.1007/s10584-014-1085-4.

Pienitz, R., Bouchard, F., Narancic, B., Vincent, W.F., and Sarrazin, D. 2017. Seasonal ice cover and catchment changes at northern thermokarst ponds in Nunavik: observations from automated time-lapse cameras, v. 1.1 (2014–2016). Nordicana. **D24**: doi: 10.5885/45418AD-AF6A8064C702444B.

Prowse, T., Alfredsen, K., Beltaos, S., Bonsal, B.R., Bowden, W.B., Duguay, C.R., Korhola, A., McNamara, J., Vincent, W.F., et al. 2011. Effects of changes in arctic lake and river ice. Ambio. **40**: 63–74. doi: 10.1007/s13280-011-0217-6.

Roiha, T., Laurion, I., and Rautio, M. 2015. Carbon dynamics in highly heterotrophic subarctic thaw ponds. Biogeosciences. **12**: 7223–7237. doi: 10.5194/bg-12-7223-2015.

Rossi, P., Laurion, I., and Lovejoy, C. 2013. Distribution and identity of bacteria in subarctic permafrost thaw ponds. Aquat. Microb. Ecol. **69**: 231–245. doi: 10.3354/ame01634.

Shirokova, L.S., Pokrovsky, O.S., Kirpotin, S.N., and Dupré, B. 2009. Heterotrophic bacterio-plankton in thawed lakes of the northern part of Western Siberia controls the CO_2 flux to the atmosphere. Int. J. Environ. Stud. **66**: 433–445. doi: 10.1080/00207230902758071.

Smith, D.C., and Azam, F. 1992. A simple, economical method for measuring bacterial protein synthesis rates in seawater using 3H-leucine. Mar. Microb. Food Webs. **6**: 107–114.

Staehr, P.A., Bade, D., Van de Bogert, M.C., Koch, G.R., Williamson, C., Hanson, P., Cole, J.J., and Kratz, T. 2010. Lake metabolism and the diel oxygen technique: state of the science. Limnol. Oceanogr. Methods. **8**: 628–644. doi: 10.4319/lom.2010.8.628.

Stefanovic, D.L., and Stefan, H.G. 2002. Two-dimensional temperature and dissolved oxygen dynamics in the littoral region of an ice-covered lake. Cold Reg. Sci. Technol. **34**: 159–178.

Terzhevik, A.Y., Pal'shin, N.I., Golosov, S.D., Zdorovennov, R.E., Zdorovennova, G.E., Mitrokhov, A.V., Potakhin, M.S., Shipunova, E.A., and Zverev, I.S. 2010. Hydrophysical aspects of oxygen regime formation in a shallow ice-covered lake. Water Res. **37**: 662–673. doi: 10.1134/S0097807810050064.

Utley, B.C., Vellidis, G., Lowrance, R., and Smith, M.C. 2008. Factors affecting sediment oxygen demand dynamics in blackwater streams of Georgia's coastal plain. J. Am. Water Resour. Assoc. **44**: 742–753. doi: 10.1111/j.1752-1688.2008.00202.x.

van Everdingen, R.O., and Banner, J.A. 1979. Use of long-term automatic time-lapse photography to measure the growth of frost blisters. Can. J. Earth Sci. **16**: 1632–1635. doi: 10.1139/e79-149.

Van Hove, P., Belzile, C., Gibson, J.A.E., and Vincent, W.F. 2006. Coupled landscape-lake evolution in the Canadian High Arctic. Can. J. Earth Sci. **43**: 533–546. doi: 10.1139/E06-003.

Vincent, W.F., Pienitz, R., and Laurion, I. 1998. Arctic and Antarctic lakes as optical indicators of global change. Ann. Glaciol. **27**: 691–696. doi: 10.3198/1998AoG27-1-691-696.

Vincent, W.F., Pienitz, R., Laurion, I., and Walter-Anthony, K. 2013. Climate impacts on Arctic lakes. *In* Climatic change and global warming of Inland waters: impacts and mitigation for ecosystems and societies. *Edited by* C.R. Goldman, M. Kumagai, and R.D. Robarts. Wiley, Chichester, UK. pp. 27–42.

Vincent, W.F., Lemay, M., and Allard, M. 2017. Arctic permafrost landscapes in transition: towards an integrated Earth system approach. Arct. Sci. **3**: This issue. doi: 10.1139/AS-2016-0027.

Vonk, J.E., Tank, S.E., Bowden, W.B., Vincent, W.F., Alekseychik, P., Amyot, M., Billet, M.F., Canário, J., Cory, R.M., et al. 2015. Effects of permafrost thaw on arctic aquatic ecosystems. Biogeosciences. **12**: 7129–7167. doi: 10.5194/bg-12-7129-2015.

Watanabe, S., Laurion, I., Pienitz, R., Chokmani, K., and Vincent, W.F. 2011. Optical diversity of thaw lakes in discontinuous permafrost: a model system for water color analysis. J. Geophys. Res. Biogeosci. **116**: G02003. doi: 10.1029/2010JG001380.

Williamson, C.E., Saros, J.E., Vincent, W.F., and Smol, J.P. 2009. Lakes and reservoirs as sentinels, integrators, and regulators of climate change. Limnol. Oceanogr. **54**: 2273–2282. doi: 10.4319/lo.2009.54.6_part_2.2273.

Wobus, C., Anderson, R., Overeem, I., Matell, N., Clow, G., and Urban, F. 2011. Thermal erosion of a permafrost coastline: improving process-based models using time-lapse photography. Arct. Antarct. Alp. Res. **43**: 474–484. doi: 10.1657/1938-4246-43.3.474.